N-TYPE CZ-SILICON SOLAR CELLS WITH SCREEN-PRINTED ALLUMINUM-ALLOYED REAR EMITTER

Robert Bock[1], Rene Hesse[1], Jan Schmidt[1], Rolf Brendel[1], Johannes Maier[2], Bert Geyer[3], Jonas Koopmann[3], and Harald Kerp[4]

[1]Institute for Solar Energy Research Hamelin (ISFH), Am Ohrberg 1, 31860 Emmerthal, Germany
[2]centrotherm photovoltaics technology GmbH, Max-Stromeyerstr. 57, 78467 Konstanz, Germany
[3]Solland Solar Cells GmbH, Bohr 10 – Avantis, 52072 Aachen, Germany
[4]Ferro GmbH Electronic Material Systems, Rodenbacher Chaussee 4, 63457 Hanau, Germany

ABSTRACT:
Applying an a-Si passivation layer to the rear-side of a screen-printed Al-p^+ emitter on an n^+np^+ solar cell structure fabricated on 3 Ωcm *n*-type phosphorus-doped Cz-Si, we achieve an independently confirmed conversion efficiency of 20%. In a second approach, we apply an Al_2O_3/SiN_x passivation stack to the screen-printed Al-p^+ emitter surface of our solar cells, where we demonstrate a conversion efficiency of 19.8% and a record-high open-circuit voltage of 649 mV. Furthermore, we introduce an industrial-type *n*-type Cz-Si solar cell featuring a screen-printed Al-p^+ emitter at the rear and a *selective* front surface field at the front. This cell has an area of 100 cm^2 and shows a stable conversion efficiency of 18.0%. This is the highest efficiency reported so far for an all-screen-printed *n*-type solar cell on Cz-Si without any boron diffusion.

1 INTRODUCTION

In today's industrial solar cell production lines, *p*-type Czochralski-grown silicon (Cz-Si) is the dominating mono crystalline base material, which is mainly due to the technological simplicity of the phosphorus diffusion process of the n^+ emitter. However, *n*-type Cz-Si has several advantages over *p*-type Cz-Si. Its carrier lifetime is much higher and it is stable under illumination [1,2]. This makes *n*-type Cz-Si the perfect material for the industrial production of high-efficiency solar cells. For solar cells where *n*-type Czochralski-grown silicon bulk material is used, a p^+-emitter is needed for the formation of the *pn*-junction. This p^+-region can e.g. be formed by a high-temperature boron diffusion or simply by a screen-printing process, where Al-paste is screen-printed on the Si wafer and subsequently fired in a conveyor-belt furnace, resulting in an Al-p^+ emitter. The high-temperature boron diffusion has in the past mainly been used for the fabrication of high-efficiency laboratory solar cells, because it is technologically more demanding and tends to induce crystallographic defects in the bulk material degrading its carrier lifetime [3,4]. On the other hand, there is a simple screen-printing-based process for the formation of the p^+-region which is mainly used for the formation of back surface fields (BSFs) on industrial *p*-type crystalline silicon solar cells [5,6] and also as Al-p^+ rear emitter on *n*-type crystalline silicon solar cells [7, 8]. However, the full-area metallization of the screen-printed Al-p^+ emitter causes a relatively high emitter surface recombination velocity which limits the solar cell conversion efficiency to some extent. To overcome this limiting factor, our ALU$^+$ *n*-type silicon solar cell concept is based on a surface-passivated screen-printed Al-p^+ emitter [9-12].

In the first part of the paper, we present our solar cell processes, in particular a detailed description of the processing sequence of our laboratory-type ALU$^+$ solar cell and of the all-screen-printed industrial-type solar cells is given. In the second part of the paper, we present the latest solar cell results of our laboratory-type and industrial-type solar cells.

2 SOLAR CELL PROCESSES

Laboratory-type solar cells

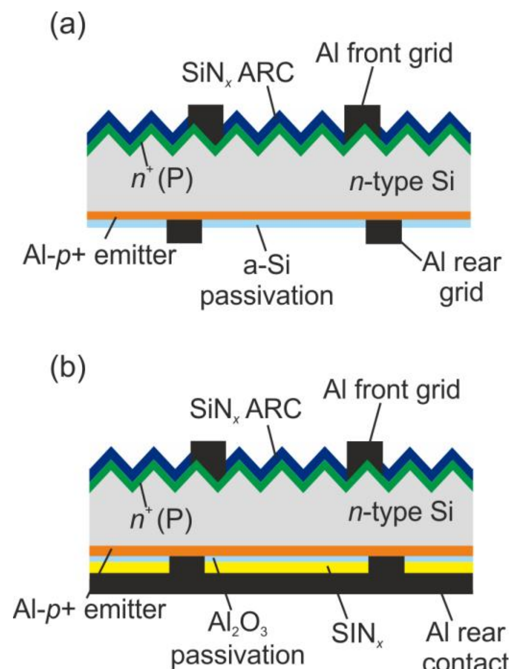

Figure 1: Two realizations of the ALU$^+$ cell concept featuring a surface-passivated screen-printed Al-p^+ emitter. (a) Evaporated Al-grid on an a-Si-passivated rear emitter [9], (b) full-area metallized Al_2O_3-passivated emitter with local point contacts (made by laser ablation).

Figure 1 shows two possible realizations of the ALU$^+$ cell with surface-passivated screen-printed Al-p^+ rear emitter [10]. The surface passivation is applied to the rear side of the cells with a locally evaporated contact grid on an a-Si passivation layer [Fig. 1 (a)], and a full-area metallized emitter featuring local point contact openings made by laser ablation for an ALD-Al_2O_3 passivation

[Fig. 1 (b)] [10].

We use (100)-oriented phosphorus-doped Czochralski-grown silicon wafers with a thickness of 190 µm and a resistivity of 3 Ωcm for our a-Si passivated solar cells and (100)-oriented 8 Ωcm phosphorus-doped float-zone (FZ) silicon wafers of 180 µm thickness for the ALD-Al_2O_3- passivated solar cells. First, we perform an n^+ front surface field (FSF) phosphorus diffusion of 100 Ω/□ into the textured diffusion windows at the front, which subsequently undergoes a wet oxidation. After the wet oxidation at 850°C we finally obtain a FSF sheet resistance of 250 Ω/□. During this oxidation the phosphorus concentration peak is mostly oxidized, resulting in an n^+ FSF with an easy-to-passivate low surface doping concentration of 3×10^{19} cm^{-3} [13,14]. After screen-printing and firing of the Al-p^+ rear emitter, the residual Al paste and the Al-Si eutectic are removed in a boiling 37% solution of HCl and the Al-p^+ emitter is etched back by 2-3 µm in a KOH solution at 70°C [9,15]. Subsequently, the wafer undergoes a further wet chemical cleaning before the emitter surface is passivated by a 20 nm thick a-Si layer deposited by means of PECVD at 225°C [see Fig. 1 (a)]. On top of the a-Si passivated cell rear we evaporate an Al contact grid through a shadow mask with a metallization fraction of 4% (finger spacing 1 mm).

The other cell type [see Fig. 1 (b)] is rear-passivated by a 30 nm thick ALD-Al_2O_3 layer which has been capped by a 150 nm thick PECVD-SiN_x layer. Subsequently, we open the rear contact points by laser ablation using a picosecond laser. After local contact opening, a full-area Al layer is evaporated on the rear side. For both cell types an Al front contact grid is evaporated through a shadow mask with a metallization fraction of ~3%. As the last process step, the SiN_x antireflection coating is deposited onto the front of both solar cell types. During the SiN_x deposition at 400°C the a-Si for the cell shown in Fig. 1 (a) underneath the Al dissolves and the Al forms an ohmic contact to the Al-p^+ emitter [16].

All-screen-printed industrial-type solar cell

Figure 2 shows a schematic representation of an industrial-type *n*-type solar cell featuring a screen-printed Al-p^+ emitter at the rear and a *local deep diffusion* (LDD) beneath the screen-printed Ag contact grid plus a weak diffusion with a low surface doping concentration between the contacts at the front. Figure 3 depicts schematically the processing sequence of the industrial-type solar cell.

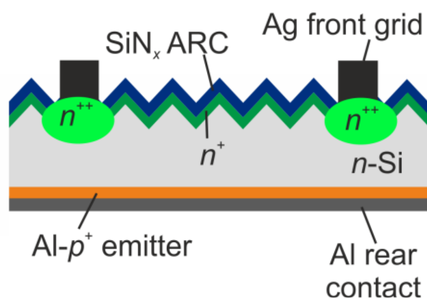

Figure 2: Schematic representation of the industrial-type solar cell featuring a local deep diffusion beneath the screen-printed Ag front grid and a fully metallized Al rear side.

The LDD beneath the Ag-contact grid serves as an effective front surface field (FSF) to the minority charge carriers and thus reduces the recombination at the Si-metal interface. Due to the locally high doping concentration at the surface it also provides an excellent ohmic contact of the screen-printed Ag-fngers to the silicon. The weak diffusion in the non-metallized front area of the cell is on the other hand shows less Auger recombination and due to the lower surface doping concentration the recombination at the surface can be reduced significantly [13,14].

The processing sequence of the solar cell is depicted schematically in Fig. 3 and will be described in detail in the following.

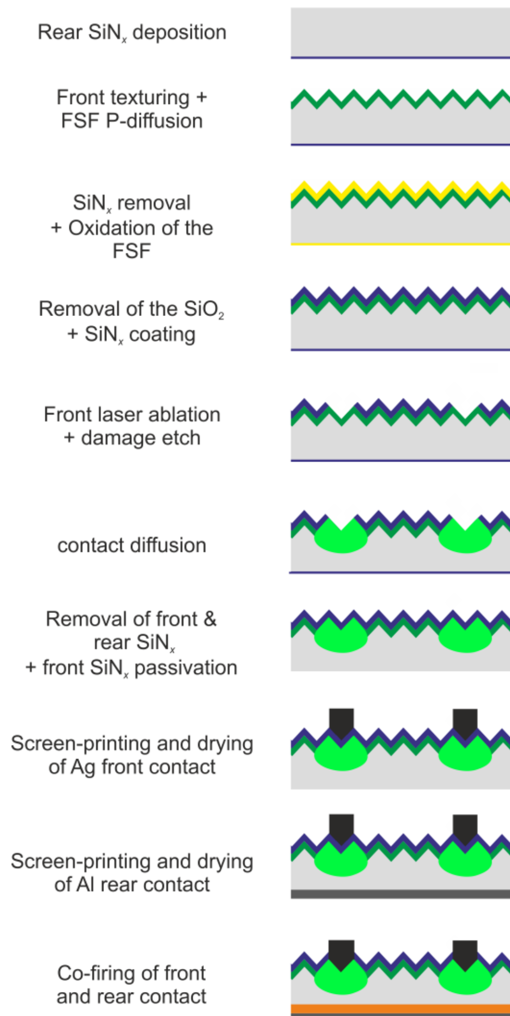

Figure 3: Processing sequence of the industrial-type *n*-type silicon solar cell featuring a screen-printed Al-p^+ rear emitter.

We use (100)-oriented phosphorus-doped Czochralski-grown silicon wafers with an initial thickness of 180 µm and a resistivity of 5 Ωcm as base material for our solar cells. The final cell thickness is 160 µm. After depositing a 150 nm thick SiN_x layer ($n = 1.9$) at the rear surface ina SiNA PECVD system (Roth & Rau), random pyramids are formed at the front side in a KOH/isopropanol solution. Then, a 80 Ω/□ phosphorus diffusion is performed the the front. Subsequently, the SiN_x at the rear and the PSG at the front are removed from the wafer by applying a short HF dip. After appling a wet oxidation at 850°C we obtain a sheet resistance of 140 Ω/□ and a low surface doping concentration of 2-4 $\times10^{19}$ cm^{-3}.

In order to protect the wafer surfaces during laser processing and the heavy contact diffusion the oxide is removed from the surface by dipping the wafers in HF and the front and rear side of the wafers are coated by a 150 nm thick SiN_x layer (n = 2.05). Then, by using a nanosecond laser the protective SiN_x is ablated from the textured front side at the positions of the future screen-printed Ag-grid. As the laser induces crystallographic defects to the silicon wafer, a damage etching for 2-3 min in an KOH solution at 90°C is performed after the laser ablation, where 3-6 µm of the silicon are removed. A phosphorus diffusion with a resulting sheet resistance of 40 Ω/□ is performed into the ablated and damage-etched areas.

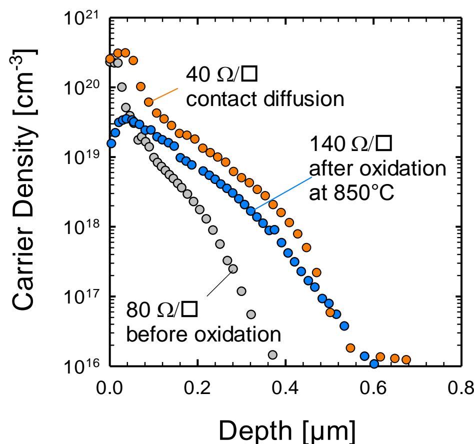

Figure 4 Doping profiles of the applied phosphorus diffusions measured with the electro chemical capacitance voltage (ECV) method.

Figure 4 shows the doping profiles of the applied phosphorus diffusions at the front measured with the electrochemical capacitance voltage (ECV) method.
Subsequent to the contact diffusion, the protective SiN_x layer is removed from the surfaces by a short HF dip and the wafers receive an RCA clean before the front side of the wafer is passivated by a 70 nm thick SiN_x layer (n = 2.05).
As the surface shows a different reflection in the laser-ablated regions compared to the textured neighbouring regions the ablated and damage-etched grid structure itself is used as alignment mark during screen-printing of the Ag grid.

Figure 5 shows an optical micrograph of a laser-ablated and damage-etched region with a screen-printed finger inside contact region region.

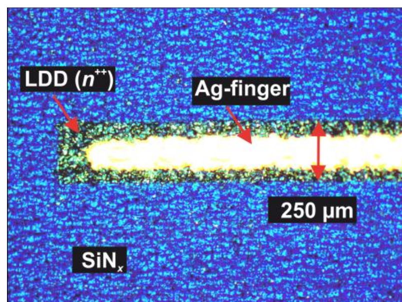

Figure 5: Optical micrograph of a Ag finger screen-printed onto an LDD region.

A glass-fritted Ag paste is screen-printed to the front side of the cell and is dried at 150°C for 4min in a belt dryer. Afterwords, a Al paste is screen-printed at the rear side of the solar cells and dried at 150°C for 10 min in a belt dryer. Finally, the solar cells are co-fred in an infrared conveyor belt furnace at a peak-firing temperature of 840°C for about 10 seconds. All screen-printing pastes used for this solar cell are comercially available.

SOLAR CELL RESUTS

Laboratory-type solar cell

The one-sun parameters of the best processed laboratory-type ALU$^+$ n-type solar cells featuring the a-Si and the Al_2O_3/SiN_x-passivated Al-p^+ emitter are summarized in Table 1. We achieve open-circuit voltages V_{oc} of 649 mV for Al_2O_3/SiN_x-passivated emitters, demonstrating the excellent emitter quality and the effective surface passivation of the Al-p^+ emitter.

The short-circuit current density of our cells is in the range of J_{sc} = 39.5 – 39.9 mA/cm^2, which confirms an effective minority-carrier diffusion to the rear junction. An energy conversion efficiency of 20.0% has been obtained for our solar cell with a-Si-passivated Al-p^+ emitter, which was independently confirmed at Fraunhofer ISE CalLab, Freiburg, Germany. The solar cell with local contact openings and a full-area metallization at the Al_2O_3/SiN_x-passivated emitter surface reaches a slightly lower cell efficiency of 19.8 %, which is mainly due to non-optimized contact openings at the rear and thus a low fill factor of 76.4%. The high short circuit current density of 39.9 mA/cm^2 is due to the increased reflection at the rear of the Al_2O_3-passivated cell.
More recently comparable cell results have been reported in other labs [17].

Table 1 ALU$^+$ solar cell parameters measured under standard testing conditions (AM1.5G, 100 mW/cm^2, 25°C) of laboratory-type ALU$^+$ solar cells. The cell area is 4 cm^2.

Passivation scheme	V_{oc} [mV]	J_{sc} [mA/cm^2]	FF [%]	η [%]
a-Si	636	39.5	79.5	**20.0***
Al_2O_3/SiN_x	649	39.9	76.4	**19.8**

*ind. confirmed at Callab

All-screen-printed industrial type solar cell

Table 2 shows the one-sun performance of our best all-screen-printed industrial-type (100 cm^2) solar cell featuring an Al-p^+ emitter at the rear and a *selective* FSF at the front measured under standard testing conditions (AM1.5G spectrum, 100 mW/cm^2, 25°C).
The open-circuit voltage amounts to V_{oc} = 625 mV and the short circuit current is J_{sc} = 36.6 mA/cm^2. The stable energy conversion effciency is η = 18.0%. The high fill factor of FF = 78.8 % indicates good contact of the screen-printed Ag-fingers at the front and also a homogeneously fired Al-p^+ emitter at the rear without any indication of shunting.

Table 2 Solar cell parameters measured under standard testing conditions (AM1.5G, 100 mW/cm^2, 25°C). Of our

best n-type Cz-Si solar cell with full-area screen-printed Al-p^+ rear emitter and *selective* FSF and Ag-screen-printed front side.

Cell area	V_{oc} [mV]	J_{sc} [mA/cm^2]	*FF* [%]	η [%]
100 cm^2	623	36.6	78.8	**18.0***

*ind. confirmed at Callab

In another batch (not shown here) we have implemented our Al_2O_3/SiN_x passivated Al-p^+ emitter to an industrial-type (100 cm^2) n^+np^+ Cz-Si solar cell structure featuring a screen-printed Ag front grid. Due to fill factor problems we have measured a conversion efficiency of only 17.6% for the best cell of this batch. However, an open-circuit voltage of V_{oc} = 643 mV has been achieved, demonstrating the high potential of the passivated and screen-printed Al-p^+ emitter for industrial-type n-type solar cells.

4 CONCLUSIONS

In this paper, we have evaluated the potential our screen-printed and passivated Al-p^+ emitter featuring an a-Si and an Al_2O_3/SiN_x surface passivation on an n^+np^+ laboratory-type (4 cm^2) solar cell structure. For our best a-Si-passivated cell, an independently confirmed conversion efficiency of 20% was obtained. The Al_2O_3/SiN_x-passivated cell shows a conversion efficiency of 19.8% and a V_{OC} of 649 mV.

We have demonstrated a conversion efficiency of 18.0 % for a large-area (100 cm^2) all-screen-printed industrial-type n-type solar cell featuring a *selective* FSF at the front. This is the highest efficiency reported so far for an all-screen-printed n-type solar cell on Cz-Si. Furthermore, we have presented a V_{oc} as high as 643 mV measured for an industrial-type solar cell on n-type Cz-Si (100 cm^2) where we had implemented the Al_2O_3/SiN_x-passivated Al-p^+ emitter.

In conclusion, our results demonstrate the high potential of the screen-printed and passivated Al-p^+ emitter for the application in high-efficient and stable n-type silicon solar cells.

ACKNOWLEDGEMENT

Funding was provided by the State of Lower Saxony and the German Ministry for the Environment, Nature Conservation and Nuclear Safety (BMU) under Contract No. 0327666.

REFERENCES

[1] J. Schmidt, A. G. Aberle, and R. Hezel, *Proc. 26th IEEE PVSC*, Anaheim, USA (1997), p.13.

[2] A. Cuevas, M. J. Kerr, C. Samundsett, F. Ferrazza, and G. Coletti, *Appl. Phys. Lett.* **81**, 4952 (2002).

[3] J. Zhao and A. Wang, *Proceedings of the 4th World Conference on Photovoltaic Energy Conversion*, Hawaii, USA (IEEE, New York, 2006) p. 996.

[4] P. J. Cousins and J. E. Cotter, *Proceedings of the 31st IEEE Photovoltaic* Specialists Conference, Orlando, USA (IEEE, New York, 2005), p. 1047.

[5] G. C. Cheek, R, P. Mertens, R. Van Overstraeten, and L. Frisson, *IEEE Trans. Electron Devices,* **ED-31**, 602 (1964).

[6] C.F. Gay, in *Proceedings of the 13th IEEE Photovoltaic Specialists Conference*, (IEEE, New York, 1978) p. 444.

[7] A. Cuevas, C. Sammundsett, M. J. Kerr, D. H. Macdonald, H. Mäckel, and P. Altermatt, *Proceedings of the 3rd World Conference on Photovoltaic Energy Conversion*, Osaka, Japan (2003), p. 963.

[8] C. Schmiga, H. Nagel, and J. Schmidt, *Prog. Photovolt.* **14**, 533 (2006).

[9] "Silicon solar cell comprising a passivated P-type surface and method for Producing the same," International Patent Application WO2010/003784 A4.

[10] R.Bock, S. Mau, J. Schmidt, B. Hoex, and R. Brendel, *IEEE Trans. Electron Devices,* **57**, no. 8, 1966 (2010).

[11] R. Bock, J. Schmidt, and R. Brendel, *Appl. Phys Lett.* **91**, 112112 (2007).

[12] R. Bock, J. Schmidt, and R. Brendel, *Phys. Stat. Sol. (RRL)* **2,** No. 6, 248-250 (2008)

[13] J. Schmidt, J.D. Moschner, J. Henze, S. Dauwe and R. Hezel, *Proceedings of the 19th European Photovoltaic Solar Energy Conference*, Paris, France (WIP, Munich, 2004), p. 391.

[14] M. J. Kerr, J. Schmidt, and A. Cuevas, J. Appl. Phys. **89**, 3821 (2001).

[15] R. Bock, J. Schmidt, R. Brendel, H. Schuhmann, and M. Seibt, *J. Appl. Phys.* **104**, 043701 (2008.).

[16] H. Plagwitz, M. Nerding, N. Ott, H.P. Strunk, and R. Brendel, *Prog. In Photovolt.: Research and Applications* **12**, 47 (2004).

[17] C. Schmiga, M. Hermle, and S. Glunz, *Proceedings of the 23rd European Photovoltaic Solar Energy Conference*, Valencia, Spain, (WIP, Munich, 2008), p. 982.